Cogn Neurodyn (2014) 8:327–334
DOI 10.1007/s11571-014-9285-1

RESEARCH ARTICLE

Random dispersion in excitatory synapse response

Francesco Ventriglia

Received: 25 October 2013 / Revised: 7 March 2014 / Accepted: 12 March 2014 / Published online: 19 March 2014

Abstract The excitatory synaptic function is subject to a huge amount of researches and fairly all the structural elements of the synapse are investigated to determine their specific contribution to the response. A model of an excitatory (hippocampal) synapse, based on time discretized Langevin equations (time-step = 40 fs), was introduced to describe the Brownian motion of Glutamate molecules (GLUTs) within the synaptic cleft and their binding to postsynaptic receptors. The binding has been computed by the introduction of a binding probability related to the hits of GLUTs on receptor binding sites. This model has been utilized in computer simulations aimed to describe the random dispersion of the synaptic response, evaluated from the dispersion of the peak amplitude of the excitatory post-synaptic current. The results of the simulation, presented here, have been used to find a reliable numerical quantity for the unknown value of the binding probability. Moreover, the same results have shown that the coefficient of variation decreases when the number of postsynaptic receptors increases, all the other parameters of the process being unchanged. Due to its possible relationships with the learning and memory, this last finding seems to furnish an important clue for understanding the basic mechanisms of the brain activity.

Keywords Glutamate synaptic response · Binding probability · EPSC peak value dispersion · Computer simulation

F. Ventriglia (✉)
Istituto di Cibernetica "E.Caianiello" del CNR, Via Campi Flegrei 34, 80078 Pozzuoli, NA, Italy
e-mail: franco@ulisse.cib.na.cnr.it

Introduction

The entire synaptic system in human brain is constituted by approximately 10^{15} synapses. About the 90 % of this system is responsible of the excitatory activity, and we can affirm that the excitatory synapse constitutes the main driving force of the brain functions. Hence, grasping what determines the time-course of its response, its variations or its random structure is of basic importance for the understanding of the brain activity. Experimental data and modeling/computational investigations made this field more and more clear, but the synaptic function still remains difficult to understand. Mathematical models—with related computer simulations analyzed almost all the known structural elements of the synapse to stress out how they contribute to shape its response (Agmon and Edelstein 1997; Diamond and Jahr 1997; Freche et al. 2011; Kleppe and Robinson 1999; Rabie et al. 2006; Savtchenko and Rusakov 2007; Stevens 2003; Trommershäuser et al. 2001; Uteshev and Pennefather 1996; Wahl et al. 1997). In a series of papers (Ventriglia and Di Maio 2000, 2003; Ventriglia 2004, 2011; Ventriglia and Di Maio 2013a, b), we formulated and investigated a mathematical model of an (hippocampal) excitatory synapse. It is based on the description of the Brownian motion of Glutamate molecules (GLUTs) within the synaptic cleft, by discrete-time Langevin equations, and of their interaction with the structural elements of the synapse, in particular with the post-synaptic receptors. The model is simulated on a parallel computer by using an ultra-fast time scale (simulation step = 40 fs). The early results of the simulation demonstrated that intrinsic random variations in basic pre-synaptic elements of the synapse can reproduce some aspects of the observed stochastic variability of the peak amplitude

of miniature excitatory post synaptic current (mEPSC) (Ventriglia and Di Maio 2000, 2003; Ventriglia 2004). Some recent simulations investigated the effects of the inclusion into the model of new data on structural elements such as the presence of filaments extending across the synaptic cleft (Araç et al. 2007; Zuber et al. 2005; Ventriglia 2011 and references therein), the (increased) size and the (lower) number of post-synaptic receptors and analyzed the consequences of the increase of the number of AMPA receptors—linked to trafficking—on the synaptic response (Ventriglia and Di Maio 2013a). The availability of more precise data on the synapse structure has been used to investigate with greater details the dynamics of the binding of Glutamate to post-synaptic receptors. Moreover, the changes induced on the time-course of the EPSC by different values of the binding probability were utilized to attribute to this important, but unknown, parameter a proper range of values (Ventriglia and Di Maio 2013b). Here, we will present and discuss the *strange* phenomenon of the peak amplitude dispersion of the synaptic response, that has been brought to light by the late simulations. This phenomenon occurs when, in a series of simulations in which all the parameters of the synaptic model remain fixed and only the seed for the initialization of the random number generator (RNG) changes, the computed mEPSC presents different amplitude peaks in various simulations. We will show that the random dispersion of the synaptic response is reduced when the number of AMPARs increases. If this computational result should reflect a corresponding neurobiological phenomenon, since the AMPARs increasing is assumed as the factor inducing the long-term potentiation (LTP), which is related to learning and memory processes, then the explanation of these two basic brain processes could change in a meaningful way.

Model of excitatory synapse

The geometry of the synaptic cleft model was based on two (concentric) cylinders with a common height of 20 nm. The entire synaptic cleft was represented by the larger one, whereas the active synaptic space was simulated by a smaller cylinder enclosed in it, having bases on the active zone (AZ) and on the post-synaptic density (PSD). Attacked on the top of AZ, a small sphere simulated a releasing neurotransmitter vesicle. AMPA and NMDA receptors were modeled as small cylinders protruding in the synaptic cleft from the PSD zone. Two small circles, having the diameter of the cross-section of a GLUT and located randomly along a circle on the exposed face of the receptors, simulated the binding sites for GLUT. The annular space, external to the AZ/PSD synaptic volume till to the boundary of the cleft, was filled with Filaments having cylindrical shape. We assumed that at the arrival of the action potential (AP), an expanding fusion pore opened within the two lipid bilayers constituting the membranes of the docked vesicle and of the top of the synaptic cleft, and put in connection the inner volume of vesicle with the synaptic cleft; it was simulated as a cylinder with a gradually increasing diameter and a fixed height (see Table 1). At the starting time of the computer simulation, $t = 0$, GLUTs contained in the vesicle were distributed in space according to an uniform distribution, while their velocity was distributed according to a Maxwell distribution. Moreover, we assumed that at this time the diameter of the fusion pore was equal to the diameter of the cross section of a GLUT, thus, the neurotransmitter molecules could start their travel to the synaptic cleft by following their Brownian motion (for more information on geometrical parameter values see "Simulation and results" herein and Ventriglia and Di Maio 2013a).

Table 1 Simulation parameters

Temperature (T)	310.16 K
Glut diffusion coefficient at 310.16 K (37 °C) (D)	$10.0 \cdot 10^{-6}$ cm^2 s^{-1}
Molecular mass of glut (m)	$2.4658025 \cdot 10^{-25}$ kg
Simulation time step (Δ)	$40 \cdot 10^{-15}$ s
Length of fusion pore (h_{pore})	12 nm
Areal pore velocity (V_{areal})	31.4 nm^2 ms^{-1}
Re-uptake probability (P_r)	$3 \cdot 10^{-6}$

Langevin equations for GLUTs Diffusion

The GLUT Brownian motion was described by Langevin equations (Gillespie 1996), which, in the discretized time form, appear as

$$\mathbf{r}_i(t+\Delta) = \mathbf{r}_i(t) + \mathbf{v}_i(t)\Delta \tag{1}$$

$$\mathbf{v}_i(t+\Delta) = \mathbf{v}_i(t) - \gamma\frac{\mathbf{v}_i(t)}{m}\Delta + \frac{\sqrt{2\epsilon\gamma\Delta}}{m}\mathbf{\Omega}_i \tag{2}$$

where $\mathbf{r}_i$ and $\mathbf{v}_i$ denote the position and the velocity of the ith molecule ($i = 1...N$; N being the total number of Glutamate molecules), Δ is the time step and $\mathbf{\Omega}_i$ is a random vector with three components, each having a Gaussian distribution with mean value $\mu = 0$ and standard deviation $\sigma = 1$. The other parameters are: m the molecular mass; γ a friction term, which depends on the absolute temperature: $\gamma = k_B\frac{T}{D}$ (k_B is the Boltzmann constant, T is the absolute temperature in Kelvin degrees, D is the diffusion coefficient of Glutamate), $\epsilon = k_BT$. The value of the diffusion coefficient D for Glutamate was computed for a temperature of 37 °C (Longsworth 1953).

The discretized Langevin equations were implemented in a parallel FORTRAN program by using message passing interface (MPI) routines. The model space was delimited by the following synaptic structures: the inner surfaces of the vesicle and the fusion pore, and, within the synaptic cleft, the pre- and post-synaptic membranes, the surface of receptors and the surface of filaments. To allow the greatest space sensibility, the space was not discretized and, for as concerns the time, an extremely short discretization step size was chosen, $\Delta = 40 \cdot 10^{-15}$ s (=40 fs). It permitted an accurate description of the collisions of GLUTs on synaptic elements. In case of impacts on the synaptic surface, the molecule was considered as a point. Conversely, in case of a collision with a hole of almost equal size of the GLUT, as the upper and lower mouths of the fusion pore or the binding sites of receptors, a spherical or ovoidal shape has been used, respectively. With regards to the absorption by pre-synaptic receptors, we supposed that GLUTs were absorbed within the synaptic cleft with a very low probability—P_R. About the spillover, we assumed that, due to the high concentration of extra-synaptic transporters on the boundary of the synapse (Gegelashvili et al. 2000), molecules reaching the boundary had no possibility to return back to the synaptic cleft space and were considered lost by the program. At each discrete time and for each molecule, the program tested whether the new computed position was such to produce a collision with some synaptic structural element and operated a reflection or an absorption, according to the case.

Hence, the paths of all the GLUTs were computed up to the occurrence of one of the following events: a re-uptake, a receptor binding or the spillover. Moreover, the computed single and double binding times between GLUTs and AMPARs/NMDARs were written in two matrices and saved on the disk to be used for the subsequent computation of the mEPSC by an external program.

The main program was run on a parallel computer, based on a cluster of four dual-processor workstations. Due to the heavy computational task, the diffusion-binding simulations were carried out for the shortest useful time, i.e. $13 \cdot 10^9$ iterations, corresponding to 520 μs (each simulation lasted 4 days). The values of the more significant parameter are reported in Table 1.

Binding probability

The necessity to investigate the binding of GLUTs to receptors by means of a probability, and not through a binding rate as usually done, is motivated by the unrealistic conditions on the Glutamate concentration within the synaptic cleft used in the experimental literature to obtain those values. In fact, the experiments carried out to analyze the binding process imposed the stationarity of the concentration of neurotransmitters within the synaptic cleft and a long period, of the order of milliseconds, of exposition of receptors to Glutamate (Clements et al. 1992; Jonas et al. 1993). Conversely, in real conditions in which the neurotransmitters are released by a docked vesicle, the flow of neurotransmitters within the cleft is far from stationarity [we can see this also from Figure 6 in Ventriglia and Di Maio (2013b)] and the diffusion process of GLUT within the synaptic cleft is much faster than supposed (100s against 1,000s of microseconds) (see Forti et al. 1997; Ventriglia 2004, 2011; Ventriglia and Di Maio 2013a).

An alternative, more exact, procedure to compute the binding of a GLUT to a macromolecule, as those which constitute the receptors, should be based on the quantum mechanics and its equations. But the complexity of this task is immediately apparent if we consider that the mass of an AMPA receptor is between 0.6 and 1.0 MDa (megadalton) (Schwenk et al. 2012); this means that an AMPAR is constituted by some tens of thousands of atoms distributed in a set of (not all known) proteins (Nakagawa 2008).

Hence, in the lack of this very difficult study we attempted a computation of the GLUT/AMPAR binding by means of a binding probability related to collisions of GLUT on AMPAR binding site, on the base of a geometrical reasoning and through comparisons of the peak amplitudes between the mEPSCs obtained by computer simulation and those experimentally recorded. We know from experimental observations that the binding takes place only in the presence of a particular arrangement of the GLUT with respect to the binding site: the GLUT is inserted into the site only when its γ-carboxyl group is ahead (Armstrong and Gouaux 2000; Sobolevsky et al. 2009; Tichelaar et al. 2004). Based on this result, we assumed in our computer simulations, that when colliding with the binding site of a receptor the GLUT had an elongated shape, as we can find in literature for Glutamate 3D structure. Moreover, to compute the binding probability we made the modeling hypothesis that the configurations producing a binding are those in which the directions of the long axis of GLUT, which point to the binding site, are restricted to a certain range of values. By considering a GLUT as a spindle set at center of a unit sphere, which encloses all the possible orientations of the molecule, we hypothesized that only the directions contained within a particular (unknown) spherical cone, are capable to produce the binding.

Hence, the binding probability was computed as the ratio between the volume of the spherical cone and that of the unit sphere and, by varying the angle of the cone—which uniquely determines the cone volume—we observed the effect of different binding probabilities on the synaptic response. Moreover, by assuming other possible, not known frictional (or quantum) elements ruling the binding,

we reduced this probability, B_P, by an arbitrary value, C_F, with $C_F = 0.2$. A further, simplifying, hypothesis was supposed: the binding to AMPA and NMDA receptors occurred with the same probability value. Because the number of AMPARs greatly exceeds that of the NMDARs, this hypothesis does not produce a meaningful distortion in the description of the dynamics of the binding process.

EPSC computation

In all our simulations only the AMPARs contributions have been considered for the computation of the mEPSC, because the ionic channels of NMDARs, being blocked by magnesium ions under normal conditions, cannot convey currents. Thus, also in the present simulations the NMDARs are considered only as competitors of AMPARs for GLUTs binding.

As in previous articles, the schema used for AMPA receptor activation was based on a Markov chain with three states, namely: Basal (B)—closed, Active (A)—open, Desensitized (D)—closed, each with three sub-states 0, 1, 2, which denoted: unbound, singly-bound and double-bound states, respectively (Clements et al. 1992; Jonas and Spruston 1994). Because we are interested mainly in the rising phase and amplitude peaks of the mEPSC, we utilized a simplified kinetic model of receptor activation, which considered only transitions occurring in a linear cascade $B_0 \rightleftharpoons B_1 \rightleftharpoons B_2 \rightleftharpoons A_2$.

Because the opening and the closing of a double-bound receptor follow probabilistic rules, the transitions between the receptor state B_2 and A_2 cause random variations in the synaptic response. When a receptor goes into the open state, it remains open for a random period of time τ_O and then it passes into the closed state and vice versa. A random variable τ_C is related to the period of closed state. The probability of receptor opening P_O is defined as the ratio between the total opening time and the sum of the total opening and total closing time. The random variables τ_O and τ_C are distributed according to the following probability density function (PDF) of exponential form $P(\tau)$:

$$P(\tau) = \alpha e^{-\alpha\tau} \tag{3}$$

with a mean value

$$\bar{\tau} = \frac{1}{\alpha}. \tag{4}$$

The values of α for the two random variables are chosen in such a way that

$$P_O = \frac{\bar{\tau}_O}{\bar{\tau}_O + \bar{\tau}_C}. \tag{5}$$

The opening probability utilized was $P_O \approx 0.83$, slightly different from the value $P_O = 0.71$, computed by Jonas et al. (1993).

Furthermore, the transitions from the closed state B_2 to the closed state B_1 obey to the law of chance and cause random variations of the synaptic response. A negative exponential distribution, with a mean value $\bar{\tau}_I$, is used for these transitions.

A specific computer program, working off line, used the AMPAR double binding times (i.e. the times at which the AMPARs went into the state B_2) to compute the random transitions to/from the state A_2 and to the state B_1 to produce single EPSC responses. The current, flowing through a generic rth AMPA receptor, was null during the closing periods, and reached a peak I_{Mr} during the opening times. The receptors did not have all the same value of the peak current, but the peak values followed a Gaussian distribution with mean value $\bar{I}_{Mr} = -1.70$ pA and $SD = 0.3$ pA. The computed synaptic response (comp-mEPSC) was obtained by adding all the single AMPA receptor currents. One-thousand mEPSC time courses were produced for each simulation. They could be considered equivalent to raw mEPSCs. Their average values were compared with mEPSCs recorded by experimental research.

Simulation and results

In a previous work, we analyzed the effects of a specific binding probability $B_P \simeq 0.0049$—related to a solid angle of 18°—with a series of five simulations, in which 154 AMPARs and 18 NMDARs were disposed on the PSD and only the initial seed of the random number generator changed. The results showed a large variance of the computed mEPSC amplitude peak, demonstrating the irregularity of the synaptic response related to this binding probability (Ventriglia and Di Maio 2013b). Moreover, in one simulation with a very large number of AMPARs (168) and a very low binding probability, $B_P \simeq 0.0015$, related to a spherical cone angle of 10°, we calculated a mEPSC having a peak that barely reached the value of one picoAmpere (1 pA). This value is far below the lowest amplitude peak recorded by experimental setups [see Figure 4 in Forti et al. (1997)] and it demonstrated that the related B_P value does not reflect the biological reality.

These simulations have shown also the possibility to define better limits for the range of binding probabilities. To this aim, new computer simulations were carried out and the phenomenon of the synaptic response dispersion was investigated with more precision. The results are presented here.

To furnish a clear view of the guidelines of the procedure, we illustrate explicitly (and briefly) some of the physiological boundaries of the synaptic structure that can not be exceeded in the simulation. The most important

boundary is constituted by the non-saturation of the post-synaptic receptors—mainly AMPARs for our purposes—which has been observed in normally functioning synapses (Liu et al. 1999). This fact imposes that the binding probability cannot grow too much, so, it cannot reach values too near to a meaningful fraction of the unity. In fact, from Figure 7 in Ventriglia and Di Maio (2013b) one can observe that each receptor site receives much more than one hit during the neurotransmitter diffusion within the synaptic cleft (which would result in saturation if B_P was close to unity). Other physical boundaries are related to the mean amplitude of the EPSC peak, which assumes a value of about −24.5 pA (Forti et al. 1997; Liu et al. 1999),

Table 2 Variable simulation parameters

AMPARs, NMDARs	Case A	Case B
AZ radius (nm)	110.0	160.0
Synaptic cleft radius (nm)	220.0	240.0
Spacing filaments (nm)	22	20
Spacing receptors (nm)	22	20

Table 3 Variable order of EPSC amplitude peaks

Probability	Seed	EPSC peak
Qprob = 0.0170D0	985456376	−24.82
	885456376	−25.40
	156456376	−21.80
Qprob = 0.0109D0	985456376	−20.11
	885456376	−16.55
	156456376	−15.56
Qprob = 0.0062D0	985456376	−10.96
	885456376	−8.32
	156456376	−10.34

and to the value of the peak current furnished by each AMPAR when they are in the open state. Together, these two results impose strict limits on the number of AMPA receptors which, at the same time, bound neurotransmitters. Another limit is fixed by the number of AMPARs and NMDARs located on the post synaptic density (PSD). In normal conditions, they were demonstrated to be about 55, the first ones, and a bit more than 10, the NMDARs (Takumi et al. 1999). All the above conditions were considered in our computer simulations.

In an extended series of simulations we analyzed three values for the binding probability, B_P: 0.01360, 0.00874, 0.00496 (related to spherical segment angle: 30°, 24°, 18°, respectively), and, for each probability value, two values were chosen for the number of AMPARs, N_A, one normal—$N_A = 55$—and the other very high—$N_A = 154$ (the respective values for NMDARs were 13 and 18). For each couple (B_P, N_A), six simulations with different RNG seeds were accomplished, for a total of 36 computer simulations. In all these simulations the releasing vesicle was located at $X0 = 0$ (i.e. at the center of AZ) and it released 775 GLUTs. The total height of AMPARs (and NMDARs) was 17 nm, while the height of the portion protruding in the synaptic cleft was 6 nm. The other synaptic parameters changed only depending with the number of AMPARs, and their values are reported in Table 2, where Case A is related to low N_A and the case B to high N_A. A last simulation series involved a greater value for the binding probability: B_P: 0.01569 (spherical segment angle: 32°). The number of AMPARs was 55 and the NMDARs were 13.

Since we observed that within the different simulation series the order of the EPSC amplitude peaks does not depend on the value of the seeds of RNG (see Table 3, where the results of case A for only three seeds are presented), in different figures the colors of the curves were

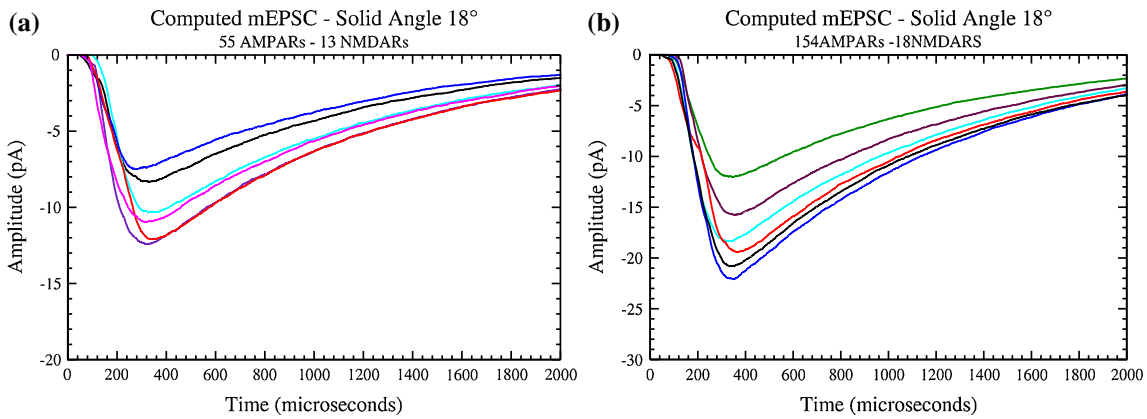

Fig. 1 **a** Low N_A, 18°, and **b** high N_A, 18°. Here, and in the following figures, the colors of the *curves* in different sub-figures do not have strict relationship with the seeds, i.e. the same color could be related to different seeds

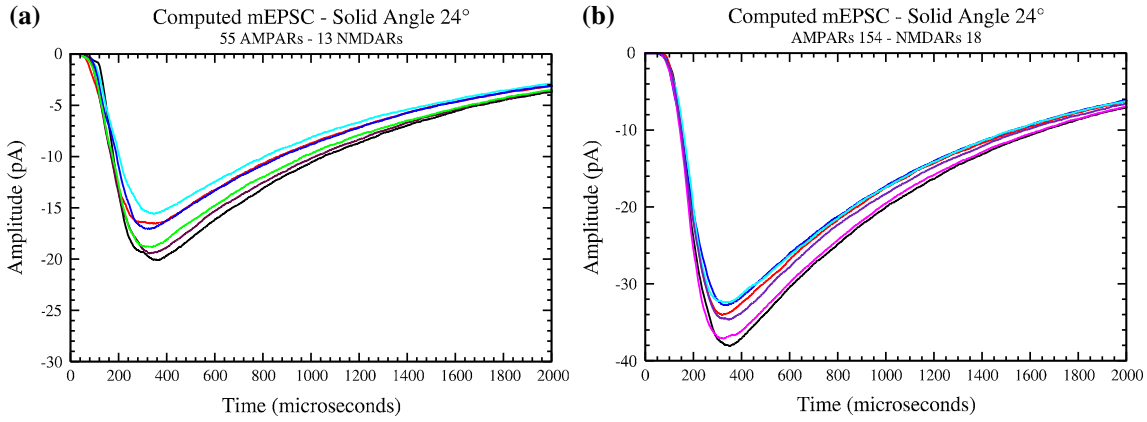

Fig. 2 **a** Low N_A, 24°, and **b** high N_A, 24°

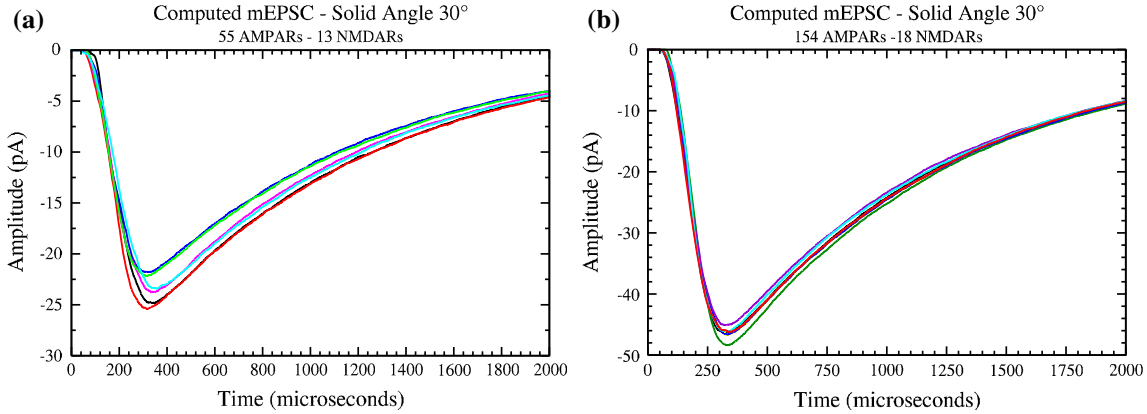

Fig. 3 **a** Low N_A, 30°, and **b** high N_A, 30°

Table 4 Amplitude peak statistics

Case	Mean value	SD	CV
Low N_A, 18°	−10.26	2.01	19.58
High N_A, 18°	−18.09	3.68	20.35
Low N_A, 24°	−17.92	1.79	10.01
High N_A, 24°	−34.85	2.31	6.62
Low N_A, 30°	−23.56	1.42	6.03
High N_A, 30°	−46.47	1.07	2.31

used without relationship with the seeds, i.e. the same color could be related to different seeds. The mEPSCs computed in all these simulations, except the last, are reported in Figs. 1, 2 and 3, while a simple statistics computed on the six mEPSCs of the six series of simulations is shown in Table 4: the mean value, the standard deviation and the CV of the amplitude peaks. The three figures are related to the three different binding probabilities and in each figure, two sub-figures present mEPSCs for the cases of normal and high number of AMPARs.

The results of simulations linked to the smallest binding probability, $B_P = 0.00496$ (solid angle 18°), are illustrated in Fig. 1, where the six curves in Fig. 1a show the time-course of the mEPSC computed for 55 AMPARs, while those in Fig. 1b have been worked out for 154 AMPARs. Both subfigures show a large dispersion of the amplitude peak of the mEPSC curves, that is also demonstrated by the related coefficient of variation (CV) in Table 4, which reaches a large value of about the 20 %. Therefore, these double results confirmed the preliminary indication of the previous work (Ventriglia and Di Maio 2013b).

The results of the test of a larger binding probability value are shown in Fig. 2. In this case the binding probability had a value $B_P = 0.008740$ (solid angle 24°). Here, both sub-figures 2a, b manifested a milder dispersion in amplitude peaks and also the CVs in Table 4 assumed smaller values of 10 and 6.6 %. What is interesting in this case, is the fact that the increase of the number of AMPARs induced a lower dispersion.

This trend was reinforced by the third couple of simulation series, that related to the largest binding probability,

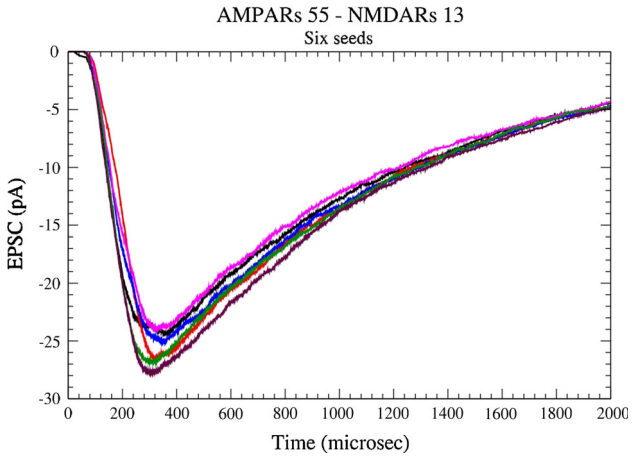

Fig. 4 Low N_A, 32°

Table 5 Amplitude peak statistics

Case	Mean value	SD	CV
Low N_A, 32°	−25.79	1.50	5.82

with a value $B_P = 0.01360$ (solid angle 30°). In fact, subfigures (a) and (b) of Fig. 3 show mEPSCs presenting a very low dispersion, while the CV reaches values of about 6 % for the lower number of AMPARs and only the 2.3 % for larger one.

The simulation of the last series was devoted to ascertain if the increasing of the binding probability could induce an even smaller CV (*Low* N_A, solid angle 32°, Fig. 4), but in this case the computed value of the CV showed only a very small decrease ($CV = 5.82$, instead of 6.02, Table 5) denoting that the CV had reached at about $B_P = 0.01360$ an almost stable value.

Discussion

The phenomenon of the peak amplitude dispersion of the synaptic response shown by some of our previous computer simulations has been analyzed in more detail in this article to ascertain possibly its origins. The aim was also to obtain information about the binding probability value of GLUTs to AMPA receptors which could furnish a better approximation to the biological reality. Several series of computer simulations have been carried out for this purpose, in each of which all the parameters of the synaptic model remained fixed and only the seed for the initialization of the RNG varied.

From the results shown in Figs. 1, 2 and 3 and Table 4 we could note that the dispersion is more marked in simulation series in which the model parameters lead to amplitude peaks with a lower mean value. The selection of a low value for the binding probability seems to be the main cause of this phenomenon. In some respects, also the presence of a lower number of AMPA receptors in the PSD contributes to increase the dispersion. We must note that the changes of the seed in RNG—all the values of the other model parameters remaining fixed—affect only the initial values of position and velocity of GLUTs within the synaptic vesicle releasing the neurotransmitter, while such values still are extracted by the same probability distributions, uniform and Maxwellian—respectively, and with the same parameters. Therefore, the large variation of the mEPSC peak amplitude shown in these particular conditions is a symptom of the instability of the synaptic response, due to too low binding probability values which were used. From these results we can conclude that the best value for an estimate of the binding probability is that related to the spherical cone angle of 30°, i.e. $B_P = 0.01360$.

The relationship between the mEPSC peak amplitude and the synaptic dispersion presents an interesting aspect, which invites to theoretical speculations. In fact, when the binding probability value is close to the superior boundary of the previously estimated binding probability range ($B_P \in [0.00496, 0.01360]$, Ventriglia and Di Maio 2013a) and the number of AMPARs is higher (*increases*), then the dispersion is reduced until it disappears. In particular, this can be observed in Fig. 3b.

This fact induces to consider the effects produced on the mEPSCs by the increasing of AMPARs that occurs in excitatory synapses during the LTP process (Anggono and Huganir 2012; Clopath 2012; Hayashi and Igarashi 2009; Malinow and Malenka 2002; Santos et al. 2009). If the reduction of the dispersion in consequence of the increased number of AMPA receptors is a phenomenon manifested also in the response of biological synapses, then the learning and the memory, which seem to be based on the LTP mechanism and on the receptor trafficking, should be considered in a different prospective. In this new view, learning and memory not only are linked to an increased value of the coupling coefficient among the neurons (i.e. of the peak amplitude of the synaptic response), but in addition they are related to a greatly reduced dispersion of the amplitude peaks with respect to that observed in normal synapses. This phenomenon is reminiscent of several other phenomena in nature, and we report, only as examples, the phase transition, as it occurs to the water, when it passes from a gaseous phase to a liquid one, or the synchronized flight of a flock of birds, or, passing to the human beings, the sudden reduction of the spectrum of behaviors which occurs in a crowd of people, attuned by some event, often a frightening one. The study of the effects of the synaptic dispersion (and of its reduction) cannot be continued only

by models of single synapses, because it requires to consider too a network of interconnected neurons. We will try to carry out the investigations by the use of our *old* model of neural population (Ventriglia 1973, 1974, 2008).

References

Agmon N, Edelstein AL (1997) Collective binding properties of receptor arrays. Biophys J 72:1582–1594

Anggono V, Huganir RL (2012) Regulation of AMPA receptor trafficking and synaptic plasticity. Curr Opin Neurobiol 22:461–469

Araç D, Boucard AA, Ozkan E, Strop P, Newell E, Südhof TC, Brunger AT (2007) Structures of neuroligin-1 and the neuroligin-1/neurexin-1 beta complex reveal specific protein–protein and protein–Ca2+ interactions. Neuron 56:992–1003

Armstrong N, Gouaux E (2000) Mechanisms for activation and antagonism of an AMPA-sensitive glutamate receptor: crystal structures of the GluR2 ligand binding core. Neuron 28:165–181

Clements JD, Lester RA, Tong J, Jahr CE, Westbrook GL (1992) The time course of glutamate in the synaptic cleft. Science 258:11498–11501

Clopath C (2012) Synaptic consolidation: an approach to long-term learning. Cogn Neurodyn 6(3):251–257

Diamond JS, Jahr CE (1997) Transporters buffer synaptically released glutamate on a submillisecond time scale. J Neurosci 17(12):4672–4687

Forti L, Bossi M, Bergamaschi A, Villa A, Malgaroli A (1997) Loose-patch recordings of single quanta at individual hippocampal synapses. Nature 388:874–878

Freche D, Pannasch U, Rouach N, Holcman D (2011) Synapse geometry and receptor dynamics modulate synaptic strength. PLoS One 6(10):e25122

Gegelashvili G, Dehnes Y, Danbolt NC, Schousboe A (2000) The high-affinity Glutamate transporters GLT1, GLAST, and EAAT4 are regulated via different signalling mechanisms. Neurochem Int 37:163–170

Gillespie DT (1996) The mathematics of Brownian motion and Johnson noise. Am J Phys 64:225–240

Hayashi H, Igarashi J (2009) LTD windows of the STDP learning rule and synaptic connections having a large transmission delay enable robust sequence learning amid background noise. Cogn Neurodyn 3(2):119–130

Jonas P, Major G, Sakmann B (1993) Quantal components of unitary EPSCs at the mossy fibre synapse on CA3 pyramidal cells of rat hippocampus. J Physiol Lond 472 C:615–663

Jonas P, Spruston N (1994) Mechanisms shaping glutamate-mediated excitatory post-synaptic currents in the CNS. Curr Opin Neurobiol 4:366–372

Kleppe IC, Robinson HP (1999) Determining the activation time course of synaptic AMPA receptors from openings of colocalized NMDA receptors. Biophys J 77:1418–1427

Liu G, Choi S, Tsien RW (1999) Variability of neurotransmitter concentration and nonsaturation of post-synaptic AMPA receptor at synapses in hippocampal cultures and slices. Neuron 22:395–409

Longsworth LG (1953) Diffusion measurements at 25°C of aqueous solutions of amino acids, peptides and sugars. J Am Chem Soc 75:5705–5709

Malinow R, Malenka RC (2002) AMPA receptor trafficking and synaptic plasticity. Annu Rev Neurosci 25:103–126

Nakagawa T (2010) The biochemistry, ultrastructure, and subunit assembly mechanism of AMPA receptors. Mol Neurobiol 42:161–184

Rabie HR, Rong J, Glavinović MI (2006) Monte Carlo simulation of release of vesicular content in neuroendocrine cells. Biol Cybern 94:483–499

Savtchenko LP, Rusakov DA (2007) The optimal height of the synaptic cleft. Proc Natl Acad Sci USA 104:1823–1828

Santos SD, Carvalho AL, Caldeira MV, Duarte CB (2009) Regulation of AMPA receptors and synaptic plasticity. Neuroscience 158:105–125

Schwenk J, Harmel N, Brechet A, Zolles G, Berkefeld H, Müller CS, Bildl W, Baehrens D, Hüber B, Kulik A, Klöcker N, Schulte U, Fakler B (2012) High-resolution proteomics unravel architecture and molecular diversity of native AMPA receptor complexes. Neuron 74:621–633

Sobolevsky AI, Rosconi MP, Gouaux E (2009) X-ray structure, symmetry and mechanism of an AMPA-subtype Glutamate receptor. Nature 462:745–756

Stevens CF (2003) Neurotransmitter release at central synapses. Neuron 40(2):381–388

Takumi Y, Matsubara A, Rinvik E, Ottersen OP (1999) The arrangement of glutamate receptors in excitatory synapses. Ann NY Acad Sci 868:474–482

Tichelaar W, Safferling M, Keinnen K, Stark H, Madden DR (2004) The three-dimensional structure of an ionotropic glutamate receptor reveals a dimer-of-dimers assembly. J Mol Biol 344:435–442

Trommershäuser J, Titz S, Keller BU, Zippelius A (2001) Variability of excitatory currents due to single-channel noise, receptor number and morphological heterogeneity. J Theor Biol 208:329–343

Uteshev VV, Pennefather PS (1996) A mathematical description of miniature post-synaptic current generation at central nervous system synapses. Biophys J 71:1256–1266

Ventriglia F (1973) Kinetic approach to neural systems. Int J Neurosci 6:29–30

Ventriglia F (1974) Kinetic approach to neural systems I. Bull Math Biol 36:535–544

Ventriglia F, Di Maio V (2000) A Brownian simulation model of glutamate synaptic diffusion in the femtosecond time scale. Biol Cybern 83:93–109

Ventriglia F, Di Maio V (2003) Stochastic fluctuations of the quantal EPSC amplitude in computer simulated excitatory synapses of hippocampus. Biosystems 71:195–204

Ventriglia F (2004) Saturation in excitatory synapses of hippocampus investigated by computer simulations. Biol Cybern 90:349–359

Ventriglia F (2008) The engram formation and the global oscillations of CA3. Cogn Neurodyn 2:335–345

Ventriglia F (2011) Effect of filaments within the synaptic cleft on the response of excitatory synapses simulated by computer experiments. Biosystems 104:14–22

Ventriglia F, Di Maio V (2013a) Effects of AMPARs trafficking and glutamate-receptors binding probability on stochastic variability of EPSC. Biosystems 112:298–304

Ventriglia F, DiMaio V (2013b) Glutamate–AMPAR interaction in a model of synaptic transmission. Brain Res 1536:168–176

Wahl LM, Pouzat C, Stratford KJ (1996) Monte Carlo simulation of fast excitatory synaptic transmission at a hippocampal synapse. J Neurophysiol 75:597–608

Zuber B, Nikonenko I, Klauser P, Muller D, Dubochet J (2005) The mammalian central nervous synaptic cleft contains a high density of periodically organized complexes. Proc Natl Acad Sci USA 102:19192–19197